DMD Fast Forward. Published on May 19, 2008 as doi:10.1124/dmd.107.019679

MS#19679

Rapid Distribution of Liposomal Short-Chain Ceramide *In Vitro* and *In Vivo*

Banu S. Zolnik, Stephan T. Stern, James M. Kaiser, Yasser Heakal, Jeffrey D. Clogston, Mark Kester and Scott E. McNeil

Nanotechnology Characterization Laboratory, Advanced Technology Program, SAIC-Frederick, Inc., NCI-Frederick, Frederick, MD 21702 (B.S.Z., S.T.S., J.D.C., S.E.M.)

Department of Pharmacology, College of Medicine, Pennsylvania State University, Hershey, PA 17033 (J.M.K., Y.H., M.K.)

Running Title: Rapid Distribution of Liposomal Short-Chain Ceramide *In Vitro* and *In Vivo*

Corresponding Author:

Stephan T. Stern

Nanotechnology Characterization Laboratory, Advanced Technology Program, SAIC-Frederick, Inc., NCI-Frederick, Frederick, MD 21702

Phone: 301-846-6198; Fax: 301-846-6399

Email: sternstephan@mail.nih.gov

Number of text pages: 21

Number of tables: 4

Number of figures: 3

Number of references: 27

Number of words in Abstract: 250

Number of words in Introduction: 547

Number of words in Discussion: 1672

Abbreviations: PEG, polyethylene glycol; RES, reticulo-endothelial system; DSPC, 1,2-distearyl-sn-glycero-3-phosphocholine; DOPE,1,2-dioleoyl-sn -glycero-3-phosphoethanolamine; C6-ceramide, N-hexanoyl-D-erythrosphingosine; AUC, area under the time concentration curve; CL, clearance; Vd, apparent volume of distribution; C_o, concentration at time zero; $t_{1/2}$, plasma half-life; MLV, multilamellar vesicle.

DMD Fast Forward. Published on May 19, 2008 as DOI: 10.1124/dmd.107.019679
This article has not been copyedited and formatted. The final version may differ from this version.

Abstract

Ceramide, an endogenous sphingolipid, has demonstrated antineoplastic activity *in vitro* and *in vivo*. However, the chemotherapeutic utility of ceramide is limited, due to its insolubility. To increase the solubility of ceramide, liposomal delivery systems have been utilized. The objective of the present study was to characterize the pharmacokinetics and tissue distribution of C6-ceramide and control (non-C6-ceramide) nanoliposomes in rats, using [^{14}C]-C6-ceramide and [^{3}H]-DSPC (distearylphosphatidylcholine) as tracers of the ceramide and liposome components, respectively. Ceramide liposomes were administered at 50 mg liposome/kg by jugular vein to female S.D. rats. The apparent volume of distribution (Vd) of [^{3}H]-DSPC was 50 mL/kg, suggesting that liposome was confined to the systemic circulation. By contrast, the Vd of [^{14}C]-C6-ceramide was 20-fold greater than that of liposome, indicating extensive tissue distribution. This high Vd of [^{14}C]-C6-ceramide in relation to [^{3}H]-DSPC suggests that ceramide and liposome distribute independently of each other. This disparate disposition was confirmed by tissue distribution studies, in which [^{14}C]-C6-ceramide exhibited rapid tissue accumulation in comparison to [^{3}H]-DSPC. Examination of ceramide liposome blood compartmentalization *in vitro* also demonstrated divergent partitioning, with liposome confined to the plasma fraction, and ceramide rapidly equilibrating between red blood cell and plasma fractions. A bilayer exchange mechanism for ceramide transfer is proposed to explain the results of the present study, as well as give insight into the documented anti-neoplastic efficacy of short-chain ceramide liposomes. Our studies suggest that this nanoscale PEG'ylated drug delivery

system for short-chain ceramide offers rapid tissue distribution without adverse effects for a neoplastic-selective, insoluble agent.

DMD Fast Forward. Published on May 19, 2008 as DOI: 10.1124/dmd.107.019679
This article has not been copyedited and formatted. The final version may differ from this version.

Introduction

Ceramide is an endogenous sphingolipid purportedly involved in cell signaling processes such as apoptosis, growth inhibition, and senescence. Ceramide is generated either by sphingomyelinase-catalyzed hydrolysis of sphingomyelin, or by *de novo* synthesis from serine and palmitoyl-CoA (Ogretmen, 2006). Endogenous long-chain ceramide levels have been shown to undergo sphingomyelinase-mediated regulation in response to external stimuli such as cytokines, hypoxia, heat, ionizing radiation, or antitumor drugs (Ogretmen and Hannun, 2004; Ogretmen, 2006). Together with ceramide's cell signaling function, these data support a therapeutic role for ceramide.

Exogenous ceramide is cytotoxic to various tumor cell lines (Shabbits and Mayer, 2003b; Stover and Kester, 2003). Long-chain (C16) ceramide has been shown to increase the life span of murine tumor models by 20% (Shabbits and Mayer, 2003a). Short-chain (C6) ceramide has also been shown effective *in vivo*, reducing murine tumor size by 6-fold (Stover et al., 2005). The therapeutic mechanism by which short-chain C6-ceramide induces tumor regression is thought to involve caspase 3/7 activation and inhibition of the Akt prosurvival pathway, resulting in DNA fragmentation and apoptosis (Stover and Kester, 2003).

Researchers have shown that ceramide, in addition to its chemotherapeutic activity, can act synergistically with existing antineoplastic agents such as paclitaxel and tamoxifen (Lucci et al., 1999; Mehta et al., 2000). This synergy may result from reversion of multi-drug resistance associated with altered ceramide metabolism. In addition to cancer therapy, ceramide may have the potential to treat a variety of other

DMD Fast Forward. Published on May 19, 2008 as DOI: 10.1124/dmd.107.019679
This article has not been copyedited and formatted. The final version may differ from this version.

conditions, such as HIV infection (Finnegan et al., 2004) and brain ischemia (Furuya et al., 2001; Zimmermann et al., 2001).

For therapeutic purposes, endogenous ceramide levels can be enhanced by increasing ceramide synthesis via induction of sphingomyelinase activity; inhibiting ceramide catabolism by blocking ceramidase activity; or by administering exogenous ceramide. The latter course is challenging, due to the inherent insolubility of ceramide, thus requiring drug delivery systems, such as liposomal formulations (Shabbits and Mayer, 2003b; Stover and Kester, 2003; Stover et al., 2005) and emulsions (Desai et al., 2007). Short-chain C6-ceramide (Figure 1), delivered as a polyethylene glycol (PEG) coated liposomal formulation, has been shown efficacious in a mouse xenograft model of human breast adenocarcinoma (Stover et al., 2005). This liposomal formulation may be expected to take advantage of passive targeting properties related to its nanoscale size and reticulo-endothelial system (RES) evading PEG coating, as has been shown for other similar liposomal formulations (Gabizon and Martin, 1997). Indeed, the pharmacokinetics of the radiolabeled [^{3}H]-C6-ceramide liposome were also investigated, and shown to follow two-compartmental first-order kinetics with sustained drug levels in the tumor tissue (Stover et al., 2005). This previous study, however, did not address the loss of liposomal drug loading *in vivo*, since the analytical methods did not differentiate between incorporated and free ceramide. From a drug delivery perspective, it is more informative to monitor both drug as well as liposomes, to gain information on the formulation's integrity/stability, since this may affect the potential therapeutic efficacy and toxicity of the drug. To better characterize the pharmacokinetics and tissue distribution of liposomal C6-ceramide, the present study examined the

DMD Fast Forward. Published on May 19, 2008 as DOI: 10.1124/dmd.107.019679
This article has not been copyedited and formatted. The final version may differ from this version.

plasma and tissue profiles of a [^{14}C]-C6 ceramide and [^{3}H]-DSPC labeled C6-ceramide nano-liposome system. The rapid, liposome independent tissue distribution of the C6-ceramide observed in these studies may have many advantages over longer-chain liposomal ceramide formulations of greater stability, but less efficient delivery.

I

DMD Fast Forward. Published on May 19, 2008 as DOI: 10.1124/dmd.107.019679
This article has not been copyedited and formatted. The final version may differ from this version.

Materials and Methods

Materials

The lipids 1,2-distearyl-sn-glycero-3-phosphocholine (DSPC), 1,2-dioleoyl-sn -glycero-3-phosphoethanolamine (DOPE), 1,2-distearoyl-sn-glycero-3-phosphoethanolamine-N-[methoxy PEG(2000)] (DSPE-PEG(2000), N-Octanoyl-Sphingosine-1-[Succinyl(Methoxy(PEG (750))] (PEG(750)-C8), N-hexanoyl-D-*erythro*-sphingosine (C6-ceramide) were purchased from Avanti Polar Lipids (Alabaster, AL). Radioactive [^{14}C]-C6-ceramide and [^{3}H]-DSPC were purchased from American Radiolabeled Chemicals (St. Louis, MO). Beckman Tissue Solubilizer 450 (BTS 450) (0.5 N quaternary ammonium hydroxide in toluene) and Ready Organic Liquid Scintillation Cocktail were purchased from Beckman Coulter (Fullerton, CA). Hydrogen peroxide and heparin sodium salt (Grade 1A: from porcine intestinal mucosa) were purchased from Sigma (St. Louis, MO). BD vacutainer, PTS gel lithium heparin plus blood collection tubes were purchased from Moore Medical (New Britain, CT). Cell Titer 96 Aqueous Non-Reactive Cell Proliferation Assay (MTS) and Apo-One Homogeneous Caspase-3/7 Assay were purchased from Promega (Madison, WI).

Liposome Formulation

PEG'ylated ceramide liposomes and control liposomes (non-C6-ceramide) were prepared as described previously, with a minor modification being the addition of radiolabeled [^{14}C]-ceramide and [^{3}H]-DSPC. (Stover et al., 2005). Briefly, lipids were solubilized in chloroform, combined in a specific molar ratio DSPC/DOPE/DSPE-PEG(2000)/PEG(750)-C8/C6-ceramide (5/2.3/1/1/4 molar ratio), dried under nitrogen,

and hydrated with sterile isotonic 0.9% NaCl solution. Control liposomes (non-C6-ceramide) contained an equivalent molar ratio of lipids as the ceramide liposome formulation. Liposomes were prepared by sonication and extrusion of the solution through 100-nm polycarbonate membranes (Stover et al., 2005). Ceramide loading in liposomes was 14 % (w/w). The specific activities of [^{14}C]-C6-ceramide and [^{3}H]-DSPC were 97.4 μCi/gram liposome and 194.8 μCi/gram liposome, respectively. The specific activity of [^{3}H]-DSPC in the control liposome was 343 μCi/gram. The liposomes were kept at 4°C in saline at a concentration of 25 mg/mL prior to use.

Particle Size Measurements

A Malvern Zetasizer Nano ZS instrument (Southborough, MA) with a backscattering detector was used for measuring the hydrodynamic size (diameter) in batch mode at 25°C in a low-volume quartz cuvette. Hydrodynamic size is reported as the volume-weighted average diameter and its percentage of the size populations present. Stock solutions of control and ceramide liposomes were diluted in PBS to give a final concentration of 1 mg/mL. A minimum of seven measurements were taken for each sample.

Zeta Potential Measurements

A Malvern Zetasizer Nano ZS instrument (Southborough, MA) was used to measure the zeta potential of control and ceramide liposomes. Samples of liposomes were diluted in 10 mM NaCl to give a 1 mg/mL final concentration. Samples were loaded into a folded capillary flow cell and a voltage of 100 V was applied. A minimum of three measurements were taken for each sample.

Pharmacokinetic and Tissue Distribution Studies

Ten-week-old double jugular catheterized female Sprague Dawley (S.D.) rats (approximate weight of 200 grams) were purchased from Charles River Laboratories (Raleigh, North Carolina). The animals were fed standard rat food (Purina) and chlorinated tap water *ad libitum*. The animal rooms were maintained on a 12-h light/dark cycle, with a temperature range between 20 and 22°C, and 50% relative humidity.

Ceramide liposomes (50 mg liposome/2 mL saline/kg) or control liposome were administered via the left jugular vein catheter (4–5 rats per treatment group). A non-liposomal C6-ceramide control group was not included, due to the insolubility of ceramide. Blood samples (200 μl) were collected via the right jugular catheters at each time point (15, 30 min, 1, 2, 4, 8, 24 and 48 h post-dose) and placed in lithium heparinized tubes. The blood was centrifuged immediately after collection, and the resulting plasma was used for pharmacokinetic (PK) analysis. For tissue distribution studies, rats were euthanized by CO_2 asphyxiation at 2 min, 1, 2 and 48 h post-dose, and the following tissues were recovered: brain, liver, lungs, kidneys, heart, and spleen.

NCI-Frederick is accredited by AAALAC International and follows the Public Health Service *Policy for the Care and Use of Laboratory Animals*. Animal care was provided in accordance with the procedures outlined in the *Guide for Care and Use of Laboratory Animals* (National Research Council, 1996; National Academy Press, Washington, D.C.).

DMD Fast Forward. Published on May 19, 2008 as DOI: 10.1124/dmd.107.019679
This article has not been copyedited and formatted. The final version may differ from this version.

Plasma and Tissue Analysis

Plasma samples: 80 µL plasma samples were mixed with one mL of BTS-450, followed by addition of 15 mL of Ready Organic Liquid Scintillation Cocktail. Tissue samples: 70–100 mg of tissue were mixed with one mL BTS-450 and incubated at 50°C for 12 h to solubilize the tissue completely. Subsequently, the samples were cooled to room temperature, treated with 200 µL of a 30% (w/w) H_2O_2 solution, and allowed to set for one h. Samples were then diluted with 15 mL of Ready Organic Liquid Scintillation Cocktail.

[^{14}C]-C6 ceramide and [^{3}H]-DSPC radioactivities were determined by scintillation counting using dual label mode (Beckman Coulter LS6500). The counting efficiencies were 50% and 80% for ^{3}H and ^{14}C, respectively. It should be noted that radioactivity measurements in tissues, blood, and plasma did not differentiate between intact tracer and metabolites derived therefrom.

Analysis of Pharmacokinetic Parameters

WinNonlin software (Pharsight Corporation) was used for non-compartmental analysis of pharmacokinetic data. Pharmacokinetic parameters were determined as follows: the area under the time concentration curve (AUC) was calculated using the linear trapezoidal rule with extrapolation to time infinity; clearance (CL) was calculated from dose/AUC; apparent volume of distribution (Vd) was calculated from dose/C_o (concentration at time zero calculated from extrapolation of the plasma time curve); plasma half-life ($t_{1/2}$) was calculated from 0.693/slope of the terminal elimination phase.

DMD Fast Forward. Published on May 19, 2008 as DOI: 10.1124/dmd.107.019679
This article has not been copyedited and formatted. The final version may differ from this version.

In Vitro Blood Interaction Studies

In vitro blood interaction studies were conducted using the blood from untreated female S.D. rats. All Eppendorf collection tubes were washed with heparin solution (70 units/mL) before adding blood. Blood samples were incubated at 37°C for 5 min before mixing with ceramide liposomes to mimic *in vivo* temperature conditions. Eppendorf tubes containing the ceramide liposome–blood mixture (liposome concentrations of 34.7, 85.4, 112.9, and 166.7 μg/mL) were incubated at 37°C for 10 min in a rotary shaker (Barnstead Thermolyte Labquake Shaker, rotation at 8 rpm) to ensure complete mixing. Following incubation, a 10-μL sample of the ceramide liposome–blood mixture was removed for radioactivity measurement. Plasma was separated from the remaining ceramide liposome–blood mixture by centrifugation (VWR Galaxy mini, 2000 *g,* 5 min), and 10 μL of the resulting plasma was used for radioactivity measurement. Plasma and blood samples were prepared by adding one mL of BTS-450 to 10 μL sample, followed by addition of 200 μL of a 30% (w/w) H_2O_2 solution and 15 mL of Ready Organic Scintillation Cocktail. Radioactivity was measured by scintillation counting using dual label mode (Beckman Coulter LS6500). The fraction of ceramide and liposome in plasma (Fp) was calculated according to Equation 1 (Weiss et al., 2006). The estimated hematocrit value (H_c) was 0.46, according to the literature (Sharp and LaRegina, 1998; Webb et al., 1998). Cp and Cb refer to concentration in plasma and in blood, respectively. All measurements were conducted in triplicate, and the mean values and standard deviations are reported.

$$F_p\% = (C_p / C_b) \times (1 - H_c) \times 100 \qquad \text{Equation 1}$$

DMD Fast Forward. Published on May 19, 2008 as DOI: 10.1124/dmd.107.019679
This article has not been copyedited and formatted. The final version may differ from this version.

Results

Particle Size Measurements

The ceramide liposomes' particle size was 123 ± 3 nm (peak corresponding to 100% based on volume-weighted average diameter). The control liposomes' particle size was 110 ± 1 nm (peak corresponding to 100% based on volume-weighted average diameter) (Supplemental Figures 1 a-b). The zeta potentials for the control and ceramide liposomes were -10.7 mV and -13.9 mV, respectively. These negative zeta potential values indicated a slight net negative surface charge for the liposomes. Extensive thermal (20-60^{0}C), long-term storage (up to 70 days at 4^{0}C) and pH (4-9) stability testing noted no significant changes in particle size (Supplemental Figures 2-4) and allude to the commercial utility (shelf-life) of this nanoscale, PEG'ylated, drug delivery system for insoluble ceramide.

Pharmacokinetic and Tissue Distribution Studies

Radiolabeled, ceramide-loaded liposomes and control liposomes were administered to S.D. rats via jugular vein catheters. The resulting plasma concentration profiles are reported as the percent injected dose per milliliter plasma for each treatment group, calculated from the amount of radioactive [^{14}C]-C6-ceramide and [^{3}H]-DSPC administered. Figure 2 shows the percent injected dose of [^{3}H]-DSPC (ceramide liposome and control liposome), and [^{14}C]-C6-ceramide per milliliter plasma vs. time profile, on the y1- and y2- axis, respectively. Pharmacokinetic parameters (C_o, AUC, CL, $t_{1/2}$ and Vd) for the ceramide, ceramide liposomes, and control liposomes are summarized in Table 1.

DMD Fast Forward. Published on May 19, 2008 as DOI: 10.1124/dmd.107.019679
This article has not been copyedited and formatted. The final version may differ from this version.

Plasma profiles (Figure 2, y-1 axis) and calculated PK parameters (Table 1) for the lipid component of the ceramide liposome and control liposome formulations were similar, indicating that ceramide incorporation did not alter liposome pharmacokinetics. By contrast, the PK parameters and plasma profile for ceramide and liposome were quite divergent. The calculated Vd for ceramide and liposomes was 1020 and 63 mL/kg, respectively. This low Vd for liposome is consistent with the systemic volume reported for rats (57.5–69.9 mL/kg) (Sharp and LaRegina, 1998), suggesting that liposomes were confined to the vasculature. The Vd of ceramide, however, was approximately 20-fold greater than the systemic volume and 2-fold greater than the total body water, implying that ceramide undergoes high tissue distribution.

Tissue distribution of [^{14}C]-C6-ceramide and [^{3}H]-DSPC were evaluated in the following organs: brain, heart, kidney, liver, lung, and spleen. The percent injected radioactive dose (% ID) per organ for [^{3}H]-DSPC ceramide liposomes, [^{3}H]-DSPC control liposomes, and [^{14}C]-C6-ceramide is shown in Tables 2a, 2b, and 2c, respectively. As with their plasma concentration profiles, tissue distribution of lipid tracer in the ceramide liposome and the control liposome groups was also comparable, demonstrating again that ceramide incorporation did not alter liposome pharmacokinetics. The [^{14}C]-C6 ceramide tissue profile mimicked the plasma profile. Approximately 23% of the injected [^{14}C]-C6 ceramide dose was accounted for in the liver at two min. In comparison to [^{14}C]-C6 ceramide, tissue accumulation of [^{3}H]-DSPC was delayed, with peak levels in liver at one h corresponding to 20% of the injected dose in both the ceramide liposome and control liposome groups.

DMD Fast Forward. Published on May 19, 2008 as DOI: 10.1124/dmd.107.019679
This article has not been copyedited and formatted. The final version may differ from this version.

Tissue distribution data was also analyzed on a per gram tissue basis in order to determine uptake selectivity relative to plasma. Tissue [^{14}C]-C6-ceramide concentrations indicated greater preferential distribution towards lung and liver, followed by heart and spleen (Table 3b). By contrast, [^{3}H]-DSPC (Table 3a) accumulated in liver and spleen only, and displayed slower tissue distribution kinetics than that of ceramide.

In Vitro Red Blood Cell Interaction Studies

In vitro studies were conducted to measure the extent of red blood cell (RBC) partitioning of the ceramide and liposome components of the ceramide liposome. Following equilibration of ceramide liposome-spiked whole blood samples at 37°C, [^{14}C]-C6 ceramide and [^{3}H]-DSPC concentrations in blood and plasma were measured. Control experiments without plasma were conducted to ensure that ceramide did not absorb to plastic, and confound results. Table 4 displays the percent of [^{14}C]-C6 ceramide and [^{3}H]-DSPC in the plasma fraction at various ceramide concentrations. These data suggest that [^{14}C]-C6 ceramide equilibrates between the plasma and blood compartments (Fp = 53–46% at 35–177 μg ceramide/mL), while the majority of the [^{3}H]-DSPC ceramide liposome remains in the plasma fraction (Fp = 91–78%, at 35–177 μg ceramide/mL).

Discussion

Ceramides, a class of sphingolipids, have been identified as potential secondary messengers in cell signaling processes. Ceramides can induce apoptosis in various tumor cell lines and have antineoplastic activity in tumor models (Stover and Kester, 2003). The chemotherapeutic utility of ceramide, however, is limited by its extremely low solubility. To overcome this limitation, liposomes consisting of one (Stover and Kester, 2003) or more (Shabbits and Mayer, 2003a) phospholipid bilayers with enclosed aqueous phases, have been used to deliver incorporated ceramide to tumors *in vivo*. Liposomal C6-ceramide has been shown to cause concentration-dependent cytotoxicity in mammary adenocarcinoma cells, with IC_{50} values of 5 μM (Stover et al., 2005). Efficacy of the liposomal C6-ceramide has also been demonstrated in a murine xenograft tumor model of human breast adenocarcinoma (Stover et al., 2005). Most intriguingly, cytotoxicity was not observed in normal epithelial cell lines at concentrations up to 50 μM (Stover et al., 2005), suggesting a neoplasm-selective mechanism. This neoplastic selective mechanism has also been observed in melanoma verses melanocytes (Tran et al., accepted) and is the basis for the untargeted, interbilayer-dependent nanoliposomal ceramide exchange delivery system used in these studies. The present study sought to further characterize the pharmacokinetics and tissue distribution of liposomal C6-ceramide in rats. The *in vivo* integrity (stability) of liposomes is an important characteristic for liposomal formulations. The drug-to-lipid ratio in plasma, relative to initial loading, can be used to determine the integrity of liposome *in vivo*. The assessment of the integrity of liposomes is crucial, since this may affect the distribution, metabolism, and excretion profile, and in turn the therapeutic efficacy and

DMD Fast Forward. Published on May 19, 2008 as DOI: 10.1124/dmd.107.019679
This article has not been copyedited and formatted. The final version may differ from this version.

toxicity of the liposomal drug. For example, premature release of drug from the liposome may result in acute toxicity. To monitor the *in vivo* integrity of liposomes, dual radiolabeled ceramide liposomes with [^{14}C]-C6-ceramide and [^{3}H]-DSPC were used in this study.

Nanotechnology drug delivery systems, such as nano-scale liposomes, have several advantages for cancer therapy (Gabizon and Martin, 1997). In particular, the prolonged circulation half-life and size-dependent distribution mechanisms of nanotechnology drug delivery systems allow for passive tumor accumulation, i.e., the enhanced permeation and retention (EPR) effect, whereby the tumor's leaky vasculature and poor lymphatic drainage result in selective tumor uptake (Iyer et al., 2006). Longer circulation time can be achieved by shielding liposomes with a PEG coating to create "stealth liposomes", thus minimizing RES uptake and enabling passive tumor targeting. As expected, PEG'ylated C6-ceramide liposomes and control liposomes exhibited a long circulation $t_{1/2}$ of 14 hours (Table 1). Also as expected, the Vd of the ^{3}H-DSPC tracer (63 mL/kg) indicated that liposomes were confined to the vasculature and did not exhibit high tissue distribution. PK parameters (C_0, AUC, CL, Vd) were similar for both ceramide liposome and control liposomal formulations, suggesting that ceramide intercalation did not alter liposome stability *in vivo*. In contrast to these results for liposomes, the Vd of ceramide was approximately 20-fold greater (1020 mL/kg), indicating a larger tissue distribution. This high tissue distribution of ceramide relative to liposome is significant and may indicate that the C6-ceramide liposomes are unstable, or more likely, that rapid release of C6-ceramide occurs and

may influence the tissue distribution, and ultimately, the therapeutic value of ceramide *in vivo*.

The nature of the ceramide/bilayer interactions could explain liposomal ceramide distribution. During the formulation of the ceramide liposome, ceramide/phospholipid bilayer interactions are favored due to ceramide's chemical structure, with small hydroxyl head group and saturated hydrophobic chains positioning themselves in the bilayer. This positioning can be envisioned as being similar to the way endogenous ceramide forms in the microdomain of the cellular bilayer membrane (Cremesti et al., 2002; Finnegan et al., 2004). It has been shown that ceramide stabilizes membranes and co-associates, forming lipid rafts (Wang and Silvius, 2003; Megha and London, 2004). Therefore, liposomal instability in the presence of ceramide is unlikely. Correspondingly, long-term storage stability studies (up to 70 days at 4°C) of ceramide liposome did not result in any particle size change, which is commonly used as an indication of instability (Supplemental Figure 3).

A likely explanation for the loss of ceramide loading *in vivo*, is that rapid ceramide transfer occurs when ceramide comes in contact with other phospholipid bilayer structures (such as red blood cells or other cell membranes) and with plasma proteins, resulting in high ceramide Vd (Figure 3). Endogenous ceramide bilayer diffusion has been studied extensively, due to its importance in cell signaling processes (Ogretmen and Hannun, 2004). In a study by Lopez-Montero et al., the half-life of ceramide bilayer diffusion in red blood cells (RBC) was reported to be rapid (within minutes). This diffusion of ceramide in RBC followed Arrhenius kinetics, where the rate of diffusion was temperature-dependent (Lopez-Montero et al., 2005). The observed preferential

distribution of ceramide to well-perfused organs, such as liver and lung (Table 3b), may be explained by this bilayer exchange mechanism. Liposome, alternatively, followed a classic RES organ uptake pattern (Table 3a).

In order to study the rapid bilayer exchange of C6-ceramide observed in the pharmacokinetic studies further, the interaction between the ceramide liposome with RBC cell membranes was investigated *in vitro*, using pooled blood samples spiked with radiolabeled ceramide liposomes. It was shown (Table 4) that approximately 50% of ceramide mass partitions into the RBC compartment under equilibrium conditions (closed system). The equilibrium was confirmed by monitoring % ceramide mass in RBC compartment at different time points (data not shown). It was not feasible to relate these *in vitro* measures of RBC partitioning to *in vivo* data, due to the difficulty of separating RBC partitioning from other rapidly occurring events such as tissue distribution. Also, the body represents an open system, thus creating difficulties in reaching equilibrium.

The literature supports the ability of lipophilic drugs to pass through the RBC membranes and equilibrate with plasma proteins (Hinderling, 1997). The role of soluble proteins, lipoproteins, and lipid exchange proteins in lipid transfer between cell membranes has been reported for cholesterol, phospholipids, sphingomyelin, alpha tocopherol, and triglycerides (Bell, 1978). For ceramide, a transbilayer diffusion in red blood cells, from the outer monolayer toward the inner monolayer, was reported to be 1 min at 20°C. This rate was too fast to be measured at 37°C (Lopez-Montero et al., 2005). Taken together, the rapid transbilayer diffusion of ceramide, and the presence of soluble lipid-associated proteins, may explain the observed equilibrium between plasma

DMD Fast Forward. Published on May 19, 2008 as DOI: 10.1124/dmd.107.019679
This article has not been copyedited and formatted. The final version may differ from this version.

and whole blood *in vitro* (Table 4). *In vitro* release assays that utilize multilamellar vesicles as a bilayer acceptor compartment have been used to better predict these interactions of liposomal drugs with red blood cells and other cell membranes *in vivo* (Shabbits et al., 2002).

The rapid release of liposomal C6-ceramide has potential advantages and disadvantages. One of the advantages of this formulation, is that rapid bilayer exchange allows for immediate distribution of ceramide to all well perfused tissues, which may not result in adverse affects as ceramide appears to exhibit a neoplasm selective mechanism. Indeed, extensive toxicology studies have shown no biologically significant changes in body weight, organ weight, clinical chemistries, hematology, gross pathology or histology at the 50 mg/kg dose level in the SD rat model, supporting a tumor selective mechanism (Detailed information of the toxicology studies of Ceramide Liposome Report can be found on the web: http://ncl.cancer.gov/working_technical_reports.asp. Last accessed January 2008). The liposomal ceramide bilayer exchange mechanism also circumvents the lysosomal degradation pathway that might be encountered following an endocytosis-mediated delivery route. On the other hand, it is desirable in cancer therapy to attain the highest concentration of the chemotherapeutic in the target tissue. Maintaining *in vivo* stability, while ensuring biologically efficacious release kinetics would further enhance selective, EPR-mediated tumor accumulation. Another potential issue is that rapid release of liposomal C6-ceramide could result in a potential disconnect between the perceived potency based on *in vitro* data, and actual *in vivo* efficacy. *In vitro* constitutes a closed

system where ceramide release directed exclusively to the target cell line, but *in vivo*, constitutes an open system with intended and unintended cellular targets.

A possible approach to prevent this rapid bilayer exchange, and better utilize the distribution related advantages inherent in nanotechnology based delivery systems might be to extend the carbon chain length of the ceramide. It has been reported that extending the carbon chain to sixteen increased this long-chain ceramide's association with liposomes (Shabbits and Mayer, 2003b). However, it should be noted that liposomal C16-ceramide cellular uptake is via an endocytosis-mediated mechanism, not bilayer exchange, which may not be as efficient and may result in lysosomal degradation. A major challenge in liposomal delivery to tumor tissue has been the lack of rapid cellular accumulation, allowing liposomes to "washout" of the interstitial space prior to incorporation of drug in the target cells, and requiring the development of targeted strategies (Hatakeyama et al., 2007). Additionally, variability in tumor vasculature "leakiness" and elevated interstitial pressure can represent a significant barrier to the initial liposome accumulation (McDonald and Baluk, 2002). In this regard, the rapid tissue distribution of the liposomal C6-ceramide may be highly advantageous in comparison to longer chain liposomal ceramide formulations of greater stability. An interesting aspect of the liposomal C6-ceramide is that even after this rapid release of ceramide from the drug delivery vehicle, the PEG'ylated nanoscale liposome (which still contains a fraction of loaded ceramide) is intact, displaying favorable kinetics and does not trigger an immunostimulatory response in animal models. Thus, the C6-ceramide liposome may also be used to deliver an encapsulated therapeutic agent that could work synergistically with ceramide.

This present study highlights the importance of monitoring the *in vivo* integrity of drug delivery platforms. Though *in vitro* testing under physiological conditions can give an initial estimate of formulation stability, realistically, it is difficult to simulate the complexity of the biological interplay found *in vivo*. This necessitates the use of analytical methodologies that can characterize the integrity of drug formulations in biological matrices, to insure that desired formulation attributes are maintained. The outcome of this approach has identified a unique drug delivery mechanism potentially responsible for the efficacy of short chain ceramide nanoliposomes despite apparent premature release of C6-ceramide from the drug delivery platform.

Acknowledgments

The authors would like to thank for Barry Neun for assistance in preparation of tissue samples for radioactivity measurements, Sarah Skoczen for assistance with particle size measurements, and Allen Kane for assistance with illustrations.

References

Bell FP (1978) Lipid exchange and transfer between biological lipid-protein structures. *Prog Lipid Res* **17:**207-243.

Cremesti AE, Goni FM and Kolesnick R (2002) Role of sphingomyelinase and ceramide in modulating rafts: do biophysical properties determine biologic outcome? *FEBS Lett* **531:**47-53.

Desai A, Vyas T and Amiji M (2007) Cytotoxicity and apoptosis enhancement in brain tumor cells upon coadministration of paclitaxel and ceramide in nanoemulsion formulations. *J Pharm Sci*.

Finnegan CM, Rawat SS, Puri A, Wang JM, Ruscetti FW and Blumenthal R (2004) Ceramide, a target for antiretroviral therapy. *Proc Natl Acad Sci U S A* **101:**15452-15457.

Furuya K, Ginis I, Takeda H, Chen Y and Hallenbeck JM (2001) Cell permeable exogenous ceramide reduces infarct size in spontaneously hypertensive rats supporting in vitro studies that have implicated ceramide in induction of tolerance to ischemia. *J Cereb Blood Flow Metab* **21:**226-232.

Gabizon A and Martin F (1997) Polyethylene glycol-coated (pegylated) liposomal doxorubicin. Rationale for use in solid tumours. *Drugs* **54 Suppl 4:**15-21.

Hatakeyama H, Akita H, Ishida E, Hashimoto K, Kobayashi H, Aoki T, Yasuda J, Obata K, Kikuchi H, Ishida T, Kiwada H, and Harashima H. (2007) Tumor targeting of doxorubicin by anti-MT1-MMP antibody-modified PEG liposomes. *Int J Pharm* **342**: 194-200.

Hinderling PH (1997) Red blood cells: a neglected compartment in pharmacokinetics and pharmacodynamics. *Pharmacol Rev* **49:**279-295.

Iyer AK, Khaled G, Fang J and Maeda H (2006) Exploiting the enhanced permeability and retention effect for tumor targeting. *Drug Discovery Today* **11:**812-818.

Lopez-Montero I, Rodriguez N, Cribier S, Pohl A, Velez M and Devaux PF (2005) Rapid transbilayer movement of ceramides in phospholipid vesicles and in human erythrocytes. *J Biol Chem* **280:**25811-25819.

Lucci A, Han TY, Liu YY, Giuliano AE and Cabot MC (1999) Modification of ceramide metabolism increases cancer cell sensitivity to cytotoxics. *International Journal Of Oncology* **15:**541-546.

McDonald DM and Baluk P (2002) Significance of blood vessel leakiness in cancer. *Cancer Res* **62**:5381-5385.

Megha and London E (2004) Ceramide Selectively Displaces Cholesterol from Ordered Lipid Domains (Rafts): Implications for Lipid Raft Structure and Function. *J. Biol. Chem.* **279:**9997-10004.

Mehta S, Blackinton D, Omar I, Kouttab N, Myrick D, Klostergaard J and Wanebo H (2000) Combined cytotoxic action of paclitaxel and ceramide against the human Tu138 head and neck squamous carcinoma cell line. *Cancer Chemotherapy And Pharmacology* **46:**85-92.

Ogretmen B (2006) Sphingolipids in cancer: regulation of pathogenesis and therapy. *FEBS Lett* **580:**5467-5476.

Ogretmen B and Hannun YA (2004) Biologically active sphingolipids in cancer pathogenesis and treatment. *Nat Rev Cancer* **4:**604-616.

Shabbits JA, Chiu GN and Mayer LD (2002) Development of an in vitro drug release assay that accurately predicts in vivo drug retention for liposome-based delivery systems. *J Control Release* **84:**161-170.

Shabbits JA and Mayer LD (2003a) High ceramide content liposomes with in vivo antitumor activity. *Anticancer Res* **23:**3663-3669.

Shabbits JA and Mayer LD (2003b) Intracellular delivery of ceramide lipids via liposomes enhances apoptosis in vitro. *Biochim Biophys Acta* **1612:**98-106.

Sharp PE and LaRegina M (1998) *The Laboratory Rat*. CRC Press.

Stover T and Kester M (2003) Liposomal delivery enhances short-chain ceramide-induced apoptosis of breast cancer cells. *J Pharmacol Exp Ther* **307:**468-475.

Stover TC, Sharma A, Robertson GP and Kester M (2005) Systemic delivery of liposomal short-chain ceramide limits solid tumor growth in murine models of breast adenocarcinoma. *Clin Cancer Res* **11:**3465-3474.

Tran M, Sharma A, Smith C, Kester M and Robertson G (Accepted) Combining nanoliposomal ceramide with sorafenib synergistically inhibits melanoma and breast cancer cell survival to decrease tumor development *Clin Cancer Res*

Wang T-Y and Silvius JR (2003) Sphingolipid Partitioning into Ordered Domains in Cholesterol-Free and Cholesterol-Containing Lipid Bilayers. *Biophys. J.* **84:**367-378.

Webb MS, Logan P, Kanter PM, St-Onge G, Gelmon K, Harasym T, Mayer LD and Bally MB (1998) Preclinical pharmacology, toxicology and efficacy of sphingomyelin/cholesterol liposomal vincristine for therapeutic treatment of cancer. *Cancer Chemother Pharmacol* **42:**461-470.

Weiss HM, Fresneau M, Camenisch GP, Kretz O and Gross G (2006) In vitro blood distribution and plasma protein binding of the iron chelator deferasirox (ICL670) and its iron complex Fe-[ICL670]2 for rat, marmoset, rabbit, mouse, dog, and human. *Drug Metab Dispos* **34:**971-975.

Zimmermann C, Ginis I, Furuya K, Klimanis D, Ruetzler C, Spatz M and Hallenbeck JM (2001) Lipopolysaccharide-induced ischemic tolerance is associated with increased levels of ceramide in brain and in plasma. *Brain Research* **895:**59-65.

DMD Fast Forward. Published on May 19, 2008 as DOI: 10.1124/dmd.107.019679
This article has not been copyedited and formatted. The final version may differ from this version.

Footnotes

This project has been funded in whole or in part with federal funds from the National Cancer Institute, National Institutes of Health, under contract N01-CO-12400. The content of this publication does not necessarily reflect the views or policies of the Department of Health and Human Services, nor does mention of trade names, commercial products, or organizations imply endorsement by the U.S. government.

The project has also been funded, in part, through the State of Pennsylvania Non-formulary Tobacco Settlement Funds. Penn State Research Foundation has licensed ceramide nanoliposomes to Tracon Pharmaceuticals, Inc., San Diego CA. MK is CMO for Keystone Nano, which develops a separate, non-liposomal ceramide nanotechnology.

DMD Fast Forward. Published on May 19, 2008 as DOI: 10.1124/dmd.107.019679
This article has not been copyedited and formatted. The final version may differ from this version.

Legends for figures

Figure 1: Chemical structure of short chain N-hexanoyl-D-erythrosphingosine (C6-Ceramide). ∗ denotes the site of ^{14}C-radiolabeled carbon

Figure 2: ^{14}C-C6 ceramide and ^{3}H-DSPC plasma profiles. Plasma time profiles are expressed as the percent injected dose per mL, (♦) ^{3}H-DSPC of ceramide liposome and (□) ^{3}H-DSPC of control liposome on y-1 axis; (●) ^{14}C-C6 ceramide on y-2 axis. Each point represents the mean ± std. dev. from n = 4-5 rats.

Figure 3: Ceramide bilayer exchange mechanism. Schematic representation of ceramide liposome and cell membrane interaction, depicting ceramide bilayer and inter-bilayer transfer.

DMD Fast Forward. Published on May 19, 2008 as DOI: 10.1124/dmd.107.019679
This article has not been copyedited and formatted. The final version may differ from this version.

Table 1

Pharmacokinetic parameters for ceramide, ceramide liposome and control liposomes. Pharmacokinetic parameters determined by noncompartmental analysis of plasma time profiles. Data are mean ± std. dev. from n = 4-5 rats.

	Co ($\mu g*mL^{-1}$)	AUC ($\mu g*hr * mL^{-1}$)	CL calculated ($mL*hr^{-1}*kg^{-1}$)	$t_{1/2}$ (hr)	V_d ($mL*kg^{-1}$)
Ceramide	7.96 ± 3.20	42.62 ± 3.60	165.19 ± 13.80	17.19 ±1.09	1020 ± 478
Ceramide Liposome	868.40 ± 325.62	14017 ± 1449	3.60 ± 0.39	14.37 ±2.21	63 ± 19
Control Liposome	787.27 ± 170.29	12802 ± 2912	4.08 ± 0.95	14.79 ±2.19	66 ± 13

DMD Fast Forward. Published on May 19, 2008 as DOI: 10.1124/dmd.107.019679
This article has not been copyedited and formatted. The final version may differ from this version.

Table 2

^{14}C-C6 ceramide and ^{3}H-DSPC tissue biodistribution. Tissue distribution data expressed as % injected dose per organ at different time points for (a) ^{3}H-DSPC ceramide liposome, (b) ^{3}H-DSPC control liposome, and (c) ^{14}C-C6 ceramide. Data are mean ± std. dev. from n = 4-5 rats.

(a)

^{3}H-DSPC Ceramide Liposome (% ID per organ)				
Tissue	2 min	1h	2 h	48 h
Plasma	89.40 ± 5.07	68.24 ± 17.29	56.52 ± 3.00	5.97 ± 1.53
Spleen	0.32 ± 0.13	1.63 ± 0.31	1.55 ± 0.44	1.53 ± 0.20
Liver	10.32 ± 0.85	19.49 ± 8.79	16.91 ± 1.17	10.71 ± 1.14
Lung	2.94 ± 1.31	1.30 ± 0.15	1.27 ± 0.34	0.66 ± 0.09
Heart	0.68 ± 0.18	0.62 ± 0.10	0.57 ± 0.03	0.32± 0.02
Kidney	1.20 ± 0.20	1.20 ± 0.11	1.46 ± 0.22	0.80 ± 0.04
Brain	0.30 ± 0.04	0.28 ± 0.04	0.31 ± 0.11	0.32 ± 0.04
Total	105.17 ± 3.67	92.76 ± 16.55	78.58 ± 3.38	20.30 ± 2.33

(b)

^{3}H-DSPC Control liposome (% ID per organ)		
Tissue	2 h	48 h
Plasma	52.48 ± 5.73	5.83 ± 2.10
Spleen	1.12 ± 0.18	0.91 ± 0.16
Liver	16.88 ± 1.88	10.03 ± 0.65
Lung	1.64 ± 0.25	0.68 ± 0.15
Heart	0.64 ± 0.08	0.33 ± 0.03
Kidney	1.20 ± 0.21	0.87 ± 0.07
Brain	0.31 ± 0.03	0.35 ± 0.10
Total	74.26 ± 5.52	19.00 ± 1.98

DMD Fast Forward. Published on May 19, 2008 as DOI: 10.1124/dmd.107.019679
This article has not been copyedited and formatted. The final version may differ from this version.

(c)

^{14}C-C6 Ceramide (% ID per organ)				
Tissue	2 min	1 h	2 h	48 h
Plasma	15.14 ± 3.79	3.54 ± 0.47	1.70 ± 0.15	0.166 ± 0.019
Spleen	0.89 ± 0.39	0.16 ± 0.01	0.09 ± 0.03	0.027 ± 0.003
Liver	22.80 ± 1.75	5.68 ± 0.84	3.88 ± 0.56	0.390 ± 0.041
Lung	8.48 ± 0.37	0.65 ± 0.13	0.29 ± 0.03	0.035 ± 0.004
Heart	1.47 ± 0.44	0.35 ± 0.02	0.11 ± 0.01	0.013 ± 0.001
Kidney	1.64 ± 0.17	1.22 ± 0.25	0.63 ± 0.07	0.048 ± 0.003
Brain	0.34 ± 0.06	0.16 ± 0.02	0.11 ± 0.01	0.036 ± 0.003
Total	50.75 ± 2.08	11.76 ± 1.11	6.82 ± 0.49	0.715 ± 0.059

DMD Fast Forward. Published on May 19, 2008 as DOI: 10.1124/dmd.107.019679
This article has not been copyedited and formatted. The final version may differ from this version.

Table 3

^{14}C-C6 ceramide and ^{3}H-DSPC tissue biodistribution. Tissue distribution data as expressed in % injected dose per gram tissue at different time points for (a) ^{3}H-DSPC ceramide liposome and (b) ^{14}C-C6 ceramide. Data are mean ± std. dev. from n =4-5 rats.

(a)

^{3}H-DSPC Ceramide Liposome (% ID per gram)				
Tissue	2 min	1h	2 h	48 h
Plasma	8.94 ± 0.51	6.82 ± 1.73	5.65 ± 0.30	0.60 ± 0.15
Spleen	0.61 ± 0.19	3.67 ± 0.43	4.23 ± 1.12	3.13 ± 0.44
Liver	1.16 ± 0.18	2.21 ± 0.82	1.82 ± 0.24	1.13 ± 0.10
Lung	1.89 ± 0.40	1.33 ± 0.22	1.26 ± 0.36	0.52 ± 0.05
Heart	0.86 ± 0.17	0.79 ± 0.06	0.72 ± 0.10	0.40 ± 0.01
Kidney	0.73 ± 0.14	0.61 ± 0.07	0.74 ± 0.15	0.43 ± 0.02
Brain	0.17 ± 0.02	0.15 ± 0.02	0.17 ± 0.06	0.17 ± 0.02

(b)

^{14}C-C6 Ceramide (% ID per gram)				
Tissue	2 min	1 h	2 h	48 h
Plasma	1.51 ± 0.38	0.35 ± 0.05	0.17± 0.02	0.017 ± 0.002
Spleen	1.66 ± 0.59	0.37 ± 0.05	0.26 ± 0.06	0.055 ± 0.003
Liver	2.56 ± 0.33	0.66 ± 0.05	0.42 ± 0.05	0.041 ± 0.004
Lung	5.74 ± 0.80	0.66 ± 0.11	0.29 ± 0.04	0.028 ± 0.002
Heart	1.85 ± 0.39	0.44 ± 0.03	0.14 ± 0.02	0.017 ± 0.001
Kidney	0.99 ± 0.12	0.62 ± 0.13	0.32 ± 0.04	0.026 ± 0.001
Brain	0.19 ± 0.03	0.09 ± 0.01	0.06 ± 0.01	0.019 ± 0.001

DMD Fast Forward. Published on May 19, 2008 as DOI: 10.1124/dmd.107.019679
This article has not been copyedited and formatted. The final version may differ from this version.

Table 4

Blood compartmentalization of ^{14}C-C6 ceramide and ^{3}H-DSPC. The percent of ^{14}C- C6 ceramide and ^{3}H-DSPC in the plasma fraction of whole blood spiked with ceramide liposome *in vitro*. Data are mean ± std. dev. from three individual determinations.

Concentration µg/mL	% in plasma	
	^{14}C- C6	^{3}H-DSPC
34.7	53 ± 4	91 ± 10
85.4	62 ± 13	99 ± 8
112.9	53 ± 9	83 ± 3
166.7	46 ± 2	78 ± 4

Figure 1

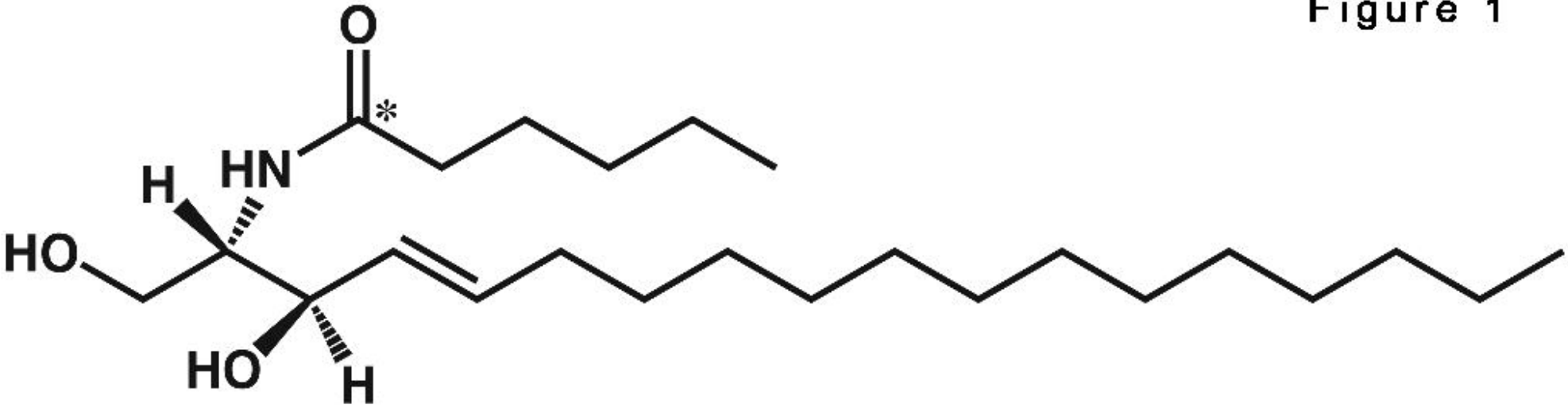

Figure 2

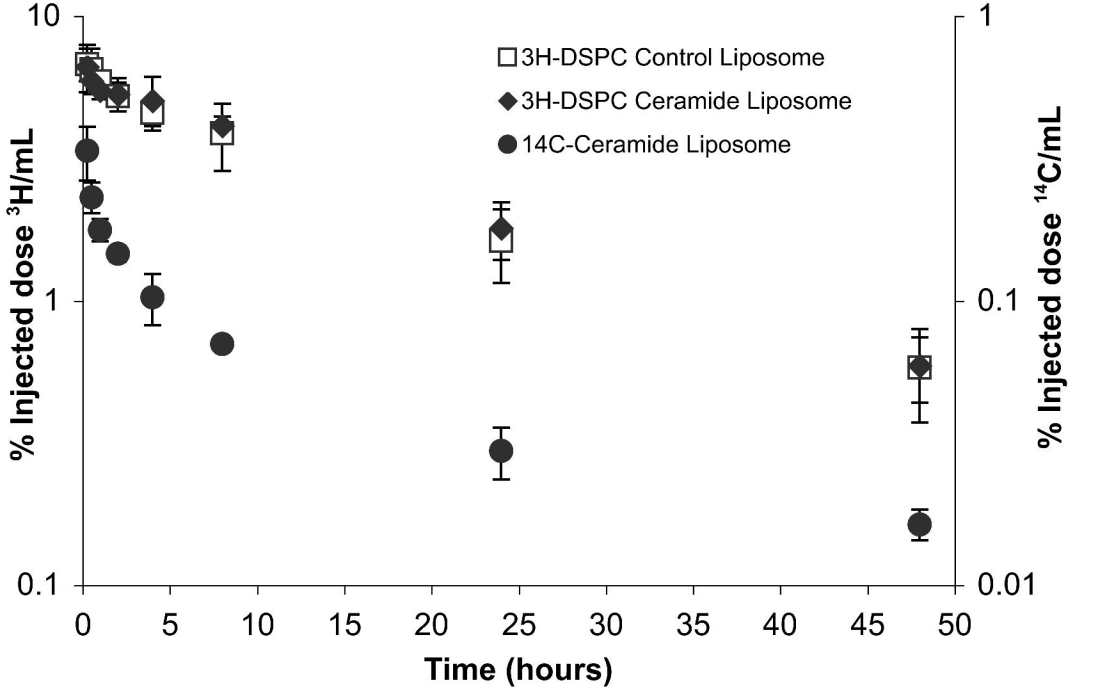
10
1
0.1
1
0.1
0.01
0
5
10
15
20
25
30
35
40
45
50
3H-DSPC Control Liposome
3H-DSPC Ceramide Liposome
14C-Ceramide Liposome
% Injected dose 3H/mL
% Injected dose 14C/mL
Time (hours)

Figure 3